Magnetic and structural properties of (Ga,Mn)As/(Al,Ga,Mn)As bilayer films

M. Wang, A. W. Rushforth, A. T. Hindmarch, R. P. Campion, K. W. Edmonds, C. R. Staddon, C. T. Foxon, and B. L. Gallagher

Magnetic and structural properties of (Ga,Mn)As/(Al,Ga,Mn)As bilayer films

M. Wang, A. W. Rushforth, A. T. Hindmarch,[a] R. P. Campion, K. W. Edmonds,
C. R. Staddon, C. T. Foxon, and B. L. Gallagher[b]
School of Physics and Astronomy, University of Nottingham, Nottingham NG7 2RD, United Kingdom

We investigate the dependence of the magnetic and structural properties of (Ga,Mn)As/(Al,Ga,Mn)As bilayer films on the stoichiometry of the interface region. For films incorporating a thin As-deficient layer at the interface, the out-diffusion of interstitial Mn from the bottom layer is strongly suppressed, resulting in a large difference in T_C and magnetic anisotropy between the two layers. X-ray reflectivity measurements show that the suppression of interstitial diffusion is correlated with an increased interface roughness. When the As-deficient interface layer is thicker than 2.5 nm, the in-plane uniaxial magnetic easy axis rotates from the [1-10] to the [110] crystalline axis. © 2013 American Institute of Physics. [http://dx.doi.org/10.1063/1.4795444]

The dilute magnetic semiconductor (Ga,Mn)As has been the subject of intense research in the field of spintronics.[1] Many of the attractive properties of (Ga,Mn)As arise from the high sensitivity of the magnetic anisotropy and the Curie temperature (T_C) to variations in the alloy concentration[1–9] or to the application of electric fields[10,11] or mechanical strain.[12–15] The sensitivity of the magnetic properties to the alloy composition opens up the possibility to grow heterostructures by molecular beam epitaxy (MBE) where different layers can have a different magnetic anisotropy and/or T_C. Such structures are useful for investigating phenomena such as tunnelling magnetoresistance (TMR),[16] tunnelling anisotropic magnetoresistance (TAMR),[17,18] and spin transfer torque (STT).[19]

A well established method to enhance the T_C of (Ga,Mn)As is to anneal, post growth, at temperatures below the growth temperature.[20,21] This allows interstitial Mn ions (Mn_I) to be removed from the lattice by diffusion of the ions to the surface where they are passivated. The Mn_I, which forms naturally during the MBE growth of the (Ga,Mn)As layers, act to compensate the charge carriers (holes) that mediate the ferromagnetic interaction and the magnetic moments of the substitutional Mn ions. Hence, removal of the Mn_I leads to an increase of T_C. The application of this technique to heterostructures requires that the interstitial Mn migrate from the buried layers through any subsequent layers in order to reach the surface of the structure. It was previously shown that both GaAs capping layers[22] and GaAs spacers in trilayer structures[23] inhibit the removal of interstitial Mn, while passivation is enhanced in thin (Ga,Mn)As layers capped with As.[24] The ability to independently remove the interstitial Mn from specific layers in a heterostructure would increase the range of possible layer combinations with desired magnetic properties that could be grown.

In this study, we investigate the out-diffusion of Mn_I in (Al,Ga,Mn)As films which are capped by a thin layer of (Ga,Mn)As. Although (Al,Ga)As is widely used in semiconductor technologies, its magnetic counterpart (Al,Ga,Mn)As has received little attention. It has been shown that the T_C

decreases with increasing concentration of Al.[3,25] Furthermore, ion channeling measurements indicated that the fraction of Mn occupying interstitial sites is increased in (Al,Ga,Mn)As compared to (Ga,Mn)As with similar total Mn concentrations.[3] Here we show that in the bilayer films, the annealing effect on the (Al,Ga,Mn)As is strongly sensitive to the detailed growth conditions in the region near the interface with the (Ga,Mn)As. In particular, we observe that a deficiency of As in this region leads to a strong suppression of Mn_I out-diffusion.

The structures investigated consist of 7 nm–10 nm $(Ga_{0.94}Mn_{0.06})As$ grown on 20 nm $(Al_{0.3}Ga_{0.66}Mn_{0.04})As$. The layers were grown by MBE on semi-insulating GaAs(001) substrates with a low temperature GaAs buffer layer. The transition from the $(Al_{0.3}Ga_{0.66}Mn_{0.04})As$ layer to the $(Ga_{0.94}Mn_{0.06})As$ layer was made by shutting off the Al flux while keeping the Ga and Mn fluxes constant. Hence, the nominal Mn percentage increases from 4% to 6%. To maintain the correct III-V stoichiometry the As pressure must also be reduced. Since the As pressure responds slowly over a period of several seconds to a reduction in the setting of the As valve, the As valve was reduced shortly before shutting off the Al flux to ensure the correct stoichiometry in the interface region. Reducing the As valve earlier resulted in a region of the $(Al_{0.3}Ga_{0.66}Mn_{0.04})As$ layer, of order a few nm thickness, that was deficient in As. We define the parameter δ as the distance below the interface at which the As valve was reduced, and the value can be calculated by multiplying the growth rate by the length of time since the As flux started to reduce until the Al flux was shut off. A range of structures for which δ was varied from 3 nm to -3 nm have been investigated (the negative value indicates that the As valve was reduced after the Al flux was shut off, resulting in an excess As flux during the initial growth of the (Ga,Mn)As layer).

The samples were characterized by measuring the magnetic properties along different crystal directions using a quantum design superconducting quantum interference device (SQUID) magnetometer. Figs. 1(a) and 1(b) show the projection of the temperature dependent remnant moment, measured after cooling in a saturating field of 1000 Oe, for two control samples consisting of 25 nm $(Al_{0.3}Ga_{0.64}Mn_{0.06})As$ and 7 nm $(Ga_{0.94}Mn_{0.06})As$, respectively, grown on GaAs(001) substrates with (Al,Ga)As buffer layers. The samples were measured as-grown and after annealing in air at 180 °C for 48 h. For

[a]Present address: Centre for Materials Physics, University of Durham, Durham DH1 3LE, United Kingdom.
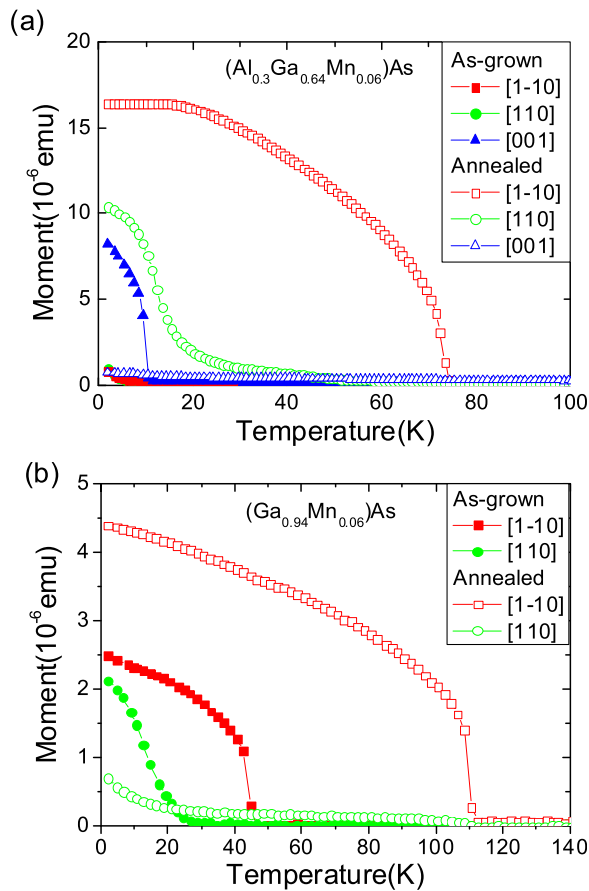[b]Author to whom correspondence should be addressed: andrew.rushforth@nottingham.ac.uk.

FIG. 1. Projection of the temperature dependent remnant moment measured after cooling in a field of 1000 Oe for (a) a 25 nm $Al_{0.3}Ga_{0.64}Mn_{0.06}As$ control sample and (b) a 7 nm $Ga_{0.94}Mn_{0.06}As$ control sample. Measurements were made along the [1–10] and [110] directions, and also the [001] direction for the $Al_{0.3}Ga_{0.64}Mn_{0.06}As$ sample in the as-grown (solid symbols) and annealed (open symbols) states, respectively.

both samples the low temperature annealing results in an increase of T_C and a modification of the magnetic anisotropy. For the $(Al_{0.3}Ga_{0.64}Mn_{0.06})As$ sample, the easy axis points out of the plane for the as-grown sample, possibly due to a strong localization of carriers due to the addition of Al.[3] After annealing the easy axis points in the plane, predominantly along the [1–10] direction over most of the temperature range. For the $(Ga_{0.94}Mn_{0.06})As$ sample, the magnetic anisotropy is in-plane.[26] It consists of a cubic component favoring easy axes along the [100] and [010] directions and a uniaxial component favoring the [1–10] direction. In common with most studied (Ga,Mn)As layers,[26,27] a spin reorientation transition is observed in the as-grown layer, with the cubic anisotropy dominating at low temperatures and the uniaxial anisotropy dominating at higher temperatures. After annealing the uniaxial anisotropy dominates over the whole temperature range.

Fig. 2(a) shows the projection of the temperature dependent remnant moment measured for a bilayer sample S1 with $\delta = 3$ nm. In the as-grown state there is a significant moment in the out of plane [001] direction at the lowest temperature. This component disappears above 5 K. There is also a component of the magnetization along the [110] direction that persists up to 49 K. After annealing (Fig. 2(c)) the component of the magnetization along the [001] direction remains, gets stronger in magnitude, and persists up to 17 K. The component of the magnetization along the [110] persists up to 96 K. By comparing to the data for the control samples (Fig. 1), we attribute the low temperature magnetization component along the [001] direction to the bottom $(Al_{0.3}Ga_{0.66}Mn_{0.04})As$ layer and the in-plane magnetization component to the top $(Ga_{0.94}Mn_{0.06})As$ layer. The effects of annealing are significantly suppressed for the bottom $(Al_{0.3}Ga_{0.66}Mn_{0.04})As$ layer, when compared to the control sample. This interpretation is confirmed by the etching study described below.

To further investigate the effects of annealing on each layer, magnetometry measurements have been performed after
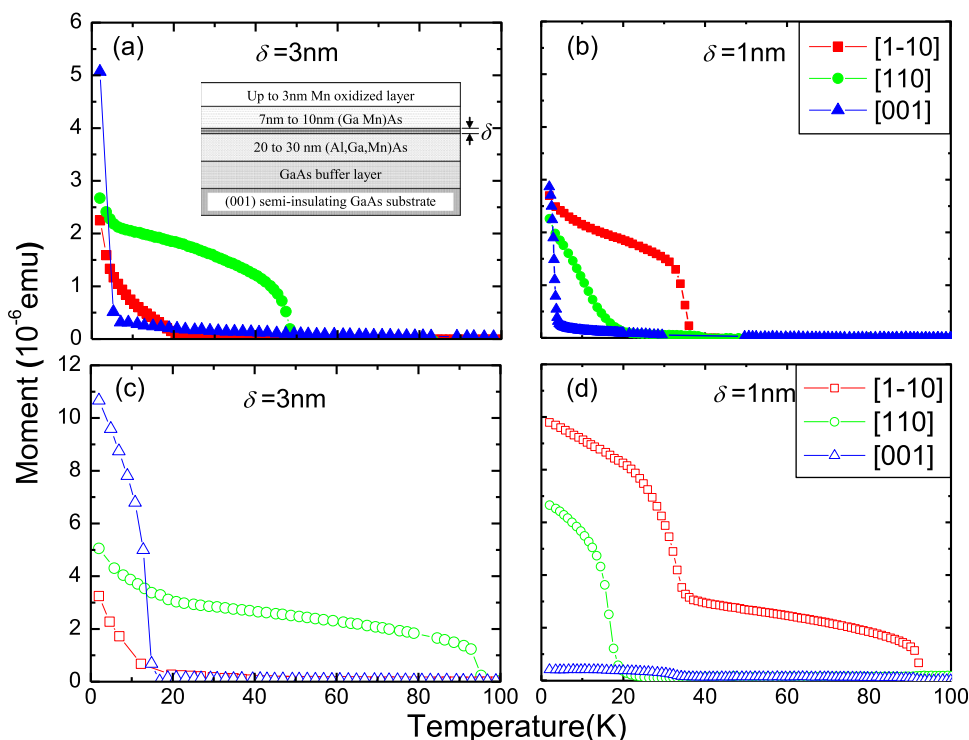

FIG. 2. Projection of the temperature dependent remnant moment after 1000 Oe field cool for bilayer samples S1 ($\delta = 3$ nm) and S2 ($\delta = 1$ nm) in the (a),(b) as grown state and (c),(d) after annealing, respectively. δ is the thickness of the As-deficient interface region. Inset on the top left: The schematic of sample structure.

etching the top surface and annealing the sample again. The etchant is 30% HCl, which is known to remove the top ≈ 1 nm of oxidized material after 30 s etching.[28] The sample was annealed at 180 °C for 10–15 h each time after etching. Fig. 3 shows that the effect of successive etching and annealing steps is to reduce the moment and T_C associated with the component of the magnetization along the [110] direction. This confirms that this component is from the top $(Ga_{0.94}Mn_{0.06})As$ layer. The reduction of T_C observed on thinning the (Ga,Mn)As layer is consistent with previous observations.[29] It is striking that the component of the magnetization along the [001] direction remains unaltered by the successive etching and annealing treatments. This remains the case until 6 etching and annealing steps have been performed, and the magnetization along the [110] direction has almost vanished (Fig. 3(c)). Upon subsequent annealing treatments the magnetization component along the [001] direction reduces, and a component along the [1–10] direction emerges with an increased T_C (Fig. 3(d)). This final trend is similar to that observed upon annealing the $(Al_{0.3}Ga_{0.64}Mn_{0.06})As$ control sample. From these observations it can be concluded that the diffusion of interstitial Mn from the bottom $(Al_{0.3}Ga_{0.66}Mn_{0.04})As$ layer is strongly suppressed until the top $(Ga_{0.94}Mn_{0.06})As$ layer is completely removed and the $(Al_{0.3}Ga_{0.66}Mn_{0.04})As$ layer surface is exposed. The top $(Ga_{0.94}Mn_{0.06})As/(Al_{0.3}Ga_{0.66}Mn_{0.04})As$ interface and the As deficient region in the top few nm of the $(Al_{0.3}Ga_{0.66}Mn_{0.04})As$ layer are the likely causes of this effect.

Figs. 2(b) and 2(d) show the projection of remnant moment measured before and after annealing, respectively, for a bilayer sample S2 with $\delta = 1$ nm. Before annealing the curves are similar to those observed for sample S1 ($\delta = 3$ nm). For the bottom $(Al_{0.3}Ga_{0.66}Mn_{0.04})As$ layer, $T_C = 4$ K and there is a perpendicular magnetic easy axis. For the top $(Ga_{0.94}Mn_{0.06})As$ layer, $T_C = 36$ K. However the easy axis is along the [1–10] direction. After annealing there are clear differences between the two samples. For sample S2 the component of the magnetization along the [001] direction is negligible after annealing, and the component along the [1–10] direction shows two clear transitions as a function of temperature. The first transition occurs at 37 K and the second at 93 K. This behavior can be explained on the basis that the interstitial Mn ions are removed from both of the layers in the heterostructure during the annealing. The first transition corresponds to T_C of the bottom $(Al_{0.3}Ga_{0.66}Mn_{0.04})As$ layer and the second transition corresponds to T_C of the top $(Ga_{0.94}Mn_{0.06})As$ layer. The bottom $(Al_{0.3}Ga_{0.66}Mn_{0.04})As$ layer has a lower T_C than the control sample because it has lower Mn concentration. Both of the layers now have the in-plane magnetic easy axis, similar to the annealed (Ga,Mn)As and (Al,Ga,Mn)As single layers.

We have studied 6 samples from 6 separate wafers with δ in the range -3 nm to 3 nm (Table I). After annealing, the characteristics of the measured remnant moment fall into two categories. Either a large moment remains along the [001] direction and a single transition is observed in the in-plane direction, indicating a suppression of the interstitial Mn out-diffusion from the bottom layer, as for samples S1, S3, and S5 or the moment along the [001] direction diminishes and two distinct transitions are observed in the magnetization in the plane, indicating that interstitial Mn can out-diffuse from the bottom layer, as for samples S2, S4, and S6. The suppression of interstitial Mn out-diffusion from the bottom layer is only found to occur for samples with $\delta \geq 2$ nm.

In order to characterize the influence of δ on the structure of the buried interface, x-ray reflectivity (XRR) measurements were performed on the six samples before and after annealing using an X'Pert materials research diffractometer system. Figs. 4(a) and 4(b) show the XRR specular scan data of annealed samples S1 and S2, respectively.

The data have been simulated by using PANalytical X'Pert Reflectivity (Version 1.1) software. This program
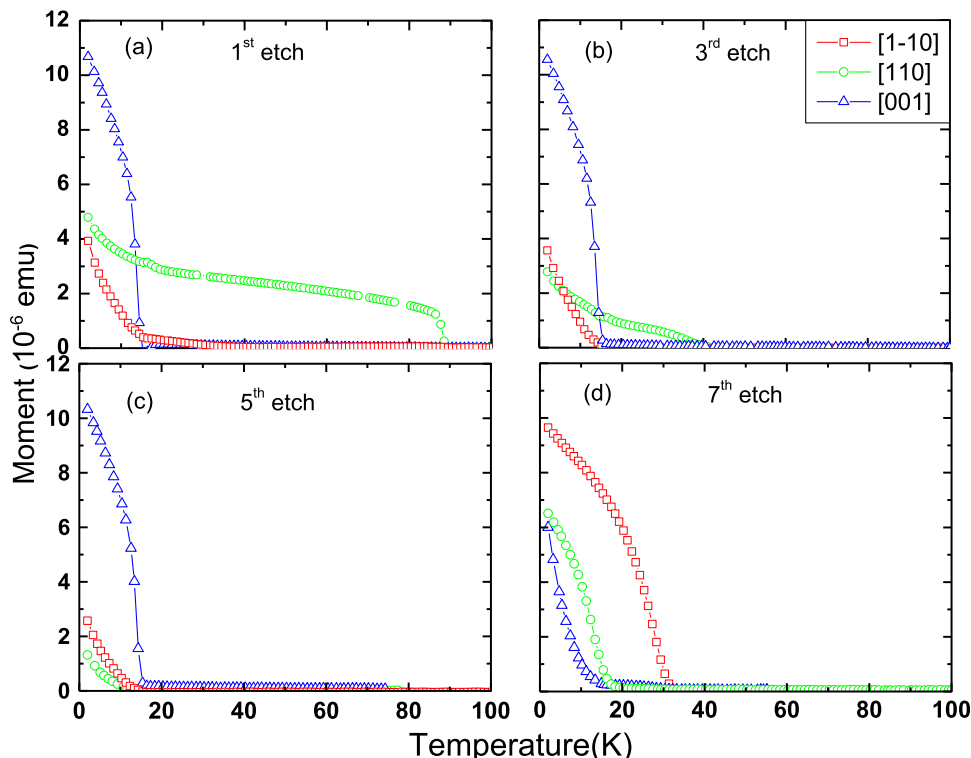

FIG. 3. Projection of the temperature dependent remnant moment after 1000 Oe field cool for bilayer sample S1 ($\delta = 3$ nm) after 1st, 3rd, 5th, 7th etch and anneal steps.

TABLE I. The T_C and anisotropy of the individual layers determined for 6 samples before and after annealing and also the (Ga,Mn)As/(Al,Ga,Mn)As interface structure obtained by x-ray reflectivity.

	Sample No.		S4	S2	S6	S5	S1	S3
Nominal δ(nm) deduced from the growth time			−3	1	1–2	2	3	3
(Ga,Mn)As	As-grown	T_C (K)	44 ± 1	37 ± 1	42 ± 1	51 ± 1	49 ± 1	54 ± 1
		Anisotropy easy axis		In plane (major: [1–10])			In plane (major: [110])	
	Annealed	T_C (K)	101 ± 1	93 ± 1	110 ± 1	92 ± 1	96 ± 1	122 ± 1
		Anisotropy easy axis		[1–10]			[110]	
Interface	As-grown	δ' (nm) from XRR	\	1.10 ± 0.05	1.25 ± 0.05	2.05 ± 0.1	2.9 ± 0.2	2.9 ± 0.1
		Interface roughness (nm)	\	∼0.1 (<0.3)	∼0.15 (<0.2)	0.5 ± 0.1	0.45 ± 0.1	0.5 ± 0.1
	Annealed	δ' (nm) from XRR	\	1.25 ± 0.1	1.25 ± 0.1	2.5 ± 0.1	3.3 ± 0.1	2.8 ± 0.1
		Interface roughness (nm)	\	∼0.2 (<0.3)	∼0.1 (<0.3)	0.5 ± 0.1	0.4 ± 0.1	0.6 ± 0.1
(Al,Ga,Mn) As	As-grown	T_C (K)	3 ± 1	4 ± 1	3 ± 1	3 ± 1	5 ± 1	5 ± 1
		Anisotropy easy axis			Out of plane [001]			
	Annealed	T_C (K)	40 ± 1	36 ± 1	44 ± 1	10 ± 1	17 ± 1	6 ± 1
		Anisotropy easy axis		In plane (major: [1–10])			Out of plane [001]	

makes use of the Parratt formalism for reflectivity,[30] and the approach used is detailed in Refs. [31] and [32]. A model in which the sample contains five layers was used. The bottom layer is the GaAs substrate plus the buffer layer, the top is a few nanometer oxidized surface, and between them are the (Al,Ga,Mn)As layer, an As deficient (Al,Ga,Mn)As layer, and the (Ga,Mn)As layer. Each layer has different parameters for material density, layer thickness, and surface or interface-roughness (root mean squared roughness (R_{RMS})), which means there are 15 parameters for the simulation. It is preferable to reduce the number of parameters for this multi-parameter simulation. Because the substrate (buffer layer) is a
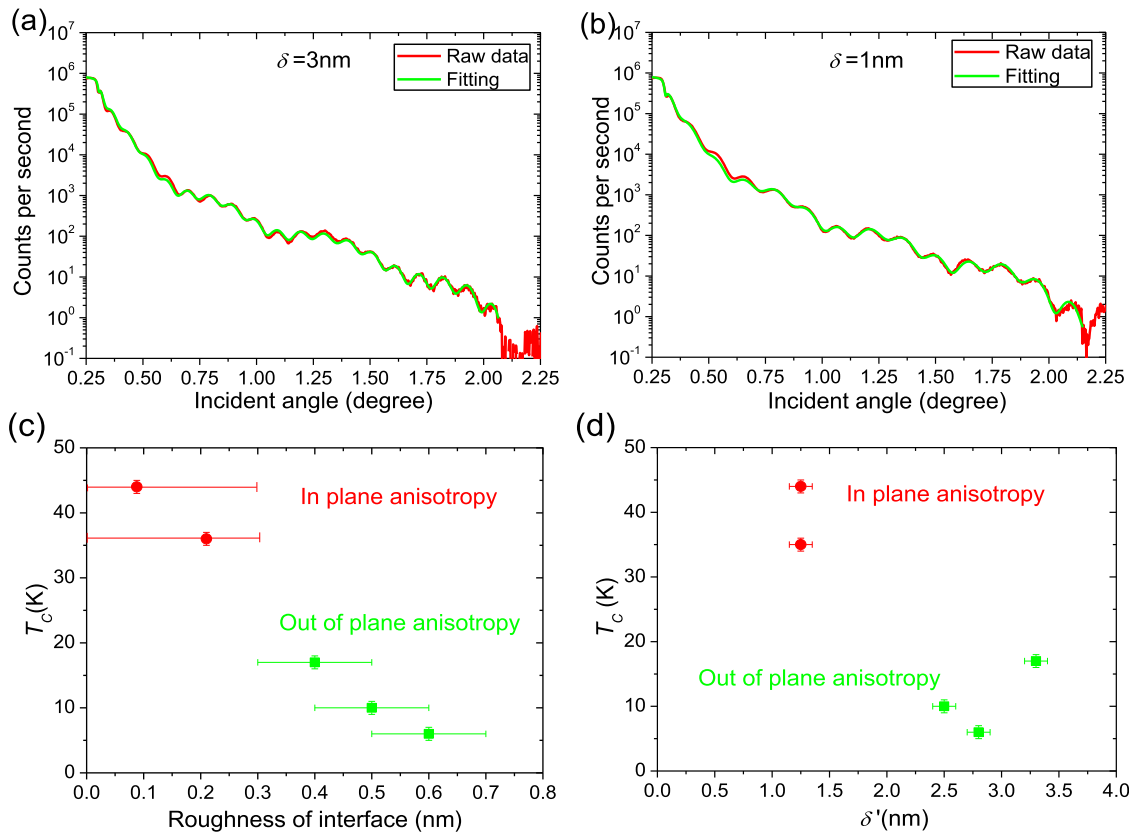
FIG. 4. X-ray reflectivity (XRR) data and simulation results for the annealed bilayer samples (a) S1 with $\delta = 3$ nm and (b) S2 with $\delta = 1$ nm; T_C of the bottom $(Al_{0.3}Ga_{0.66}Mn_{0.04})$As layer for 5 annealed samples shown as a function of (c) interface-roughness between (Ga,Mn)As and As-deficient (Al,Ga,Mn)As layers, and (d) thickness δ' of As deficient region as determined by XRR. Circles and squares are for (Al,Ga,Mn)As layers with in-plane and out-of-plane magnetic easy axes, respectively.

high quality GaAs single crystal, all the parameters of this layer can be fixed to constant values. Due to the high quality epitaxy growth, it should have a smooth interface between the As normal and As deficient (Al,Ga,Mn)As layer, which means the roughness of this interface should be close to zero. This has been proved by the simulation results which show the values of roughness at this interface are less than 0.1 nm (within the precision of XRR measurement) for all the samples.

The simulation shows similarly good fitting for most of samples except sample S4 with $\delta = -3$ nm. The reason could be that the (Ga,Mn)As layer containing excess As has a more complicated structure than other samples. The simulation results for the XRR measurements of the remaining 5 samples are shown in Table I. As shown in Fig. 4(c), there is a clear trend between the roughness of the interface between (Ga,Mn)As and (Al,Ga,Mn)As layers, and the T_C of the bottom layer for the annealed samples. In particular, suppression of interstitial Mn out-diffusion occurs when the interface-roughness is larger than a monolayer (≈ 0.3 nm). A roughening of the growth surface under As-deficient conditions is known to occur for GaAs as well as (Ga,Mn)As (Ref. 33) and may be related to the formation of deep-level defects (e.g., Ga_{As} anti-sites, Ga interstitials, or As vacancies) and Ga droplets which may become energetically favorable when there is a deficit of As. Such defects may form an electrostatic barrier close to the interface, opposing the diffusion of interstitial Mn and reducing T_C. This may explain why the T_C of the (Al,Ga,Mn)As layer after annealing is strongly correlated with the (Ga,Mn)As/(Al,Ga,Mn)As interface-roughness.

For the two films with the highest value of δ' (the thickness of As deficient (Al,Ga,Mn)As layer from XRR measurement), the uniaxial easy axis of the $(Ga_{0.94}Mn_{0.06})As$ layer lies along the [110] axis. This is in contrast to the control sample as well as the bilayer films with $\delta' < 2.5$ nm, for which the easy direction is along [1–10]. Although the origin of the uniaxial component of the anisotropy is uncertain, it has been suggested that it arises due to the direction of As bonds at the growth surface.[34] It may therefore be inferred that growing with a significant deficiency of As at the interface affects the surface reconstruction and thus the incorporation of Mn, in such a way that the [110] becomes the preferred easy axis direction. This behavior is also observed in $Co_{50}Fe_{50}$ grown on n-type GaAs.[35]

Our results show that the out-diffusion of interstitial Mn in ferromagnetic semiconductor bilayer films can be suppressed by reducing the As flux in the interface region during growth. In this way, it may be possible to tailor the magnetic properties of adjacent magnetic layers such that there are large differences in T_C and magnetic anisotropy. This will be useful for growing heterostructures with desired magnetic properties for studies of interlayer magnetotransport phenomena, such as TMR, TAMR, and STT.

[1] T. Jungwirth, J. Sinova, J. Masek, J. Kucera, and A. H. MacDonald, Rev. Mod. Phys. **78**, 809 (2006).

[2] M. Sawicki, K. Y. Wang, K. W. Edmonds, R. P. Campion, C. R. Staddon, N. R. S Farley, C. T. Foxon, E. Papis, E. Kaminska, A. Piotrowska, T. Dietl, and B. L. Gallagher, Phys. Rev. B **71**, 121302(R) (2005).

[3] A. W. Rushforth, N. R. S. Farley, R. P. Campion, K. W. Edmonds, C. R. Staddon, C. T. Foxon, B. L. Gallagher, and K. M. Yu, Phys. Rev. B **78**, 085209 (2008).

[4] A. W. Rushforth, M. Wang, N. R. S. Farley, R. P. Campion, K. W. Edmonds, C. R. Staddon, C. T. Foxon, and B. L. Gallagher, J. Appl. Phys. **104**, 073908 (2008).

[5] A. Casiraghi, A. W. Rushforth, M. Wang, N. R. S. Farley, P. Wadley, J. L. Hall, C. R. Staddon, K. W. Edmonds, R. P. Campion, C. T. Foxon, and B. L. Gallagher, Appl. Phys. Lett. **97**, 122504 (2010).

[6] A. Lemaître, A. Miard, L. Travers, O. Mauguin, L. Largeau, C. Gourdon, V. Jeudy, M. Tran, and J.-M. George, Appl. Phys. Lett. **93**, 021123 (2008).

[7] M. Cubukcu, H. J. von Bardeleben, Kh. Khazen, J. L. Cantin, O. Mauguin, L. Largeau, and A. Lemaître, Phys. Rev. B **81**, 041202 (2010).

[8] P. R. Stone, J. W. Beeman, K. M. Yu, and O. D. Dubon, Physica B **401–402**, 454 (2007).

[9] P. R. Stone, K. Alberi, S. K. Z. Tardif, J. W. Beeman, K. M. Yu, W. Walukiewicz, and O. D. Dubon, Phys. Rev. Lett. **101**, 087203 (2008).

[10] M. Sawicki, D. Chiba, A. Korbecka, Y. Nishitani, J. A. Majewski, F. Matsukura, T. Dietl, and H. Ohno, Nat. Phys. **6**, 22 (2010).

[11] I. Stolichnov, S. W. E. Riester, H. J. Trodahl, N. Setter, A. W. Rushforth, K. W. Edmonds, R. P. Campion, C. T. Foxon, B. L. Gallagher, and T. Jungwirth, Nat. Mater. **7**, 464 (2008).

[12] A. W. Rushforth, E. De Ranieri, J. Zemen, J. Wunderlich, K. W. Edmonds, C. S. King, E. Ahmad, R. P. Campion, C. T. Foxon, B. L. Gallagher, K. Vyborny, J. Kucera, and T. Jungwirth, Phys. Rev. B **78**, 085314 (2008).

[13] E. De Ranieri, A. W. Rushforth, K. Vyborny, U. Rana, E. Ahmed, R. P. Campion, C. T. Foxon, B. L. Gallagher, A. C. Irvine, J. Wunderlich, and T. Jungwirth, New J. Phys. **10**, 065003 (2008).

[14] M. Overby, A. Chernyshov, L. P. Rokhinson, X. Liu, and J. K. Furdyna, Appl. Phys. Lett. **92**, 192501 (2008).

[15] S. T. B. Goennenwein, M. Althammer, C. Bihler, A. Brandlmaier, S. Geprägs, M. Opel, W. Schoch, W. Limmer, R. Gross, and M. S. Brandt, Phys. Status Solidi (RRL) **2**, 96 (2008).

[16] R. Mattana, M. Elsen, J.-M. George, H. Jaffrès, F. N. Van Dau, A. Fert, M. F. Wyczisk, J. Olivier, P. Galtier, B. Lépine, A. Guivarc'h, and G. Jézéquel, Phys. Rev. B **71**, 075206 (2005).

[17] C. Gould, C. Rüster, T. Jungwirth, E. Girgis, G. M. Schott, R. Giraud, K. Brunner, G. Schmidt, and L. W. Molenkamp, Phys. Rev. Lett. **93**, 117203 (2004).

[18] C. Rüster, C. Gould, T. Jungwirth, J. Sinova, G. M. Schott, R. Giraud, K. Brunner, G. Schmidt, and L. W. Molenkamp, Phys. Rev. Lett. **94**, 027203 (2005).

[19] M. Elsen, O. Boulle, J.-M. George, H. Jaffrès, R. Mattana, V. Cros, A. Fert, A. Lemaitre, R. Giraud, and G. Faini, Phys. Rev. B **73**, 035303 (2006).

[20] K. W. Edmonds, K. Y. Wang, R. P. Campion, A. C. Neumann, N. R. S. Farley, B. L. Gallagher, and C. T. Foxon, Appl. Phys. Lett. **81**, 4991 (2002).

[21] K. W. Edmonds, P. Boguslawski, K. Y. Wang, R. P. Campion, S. V. Novikov, N. R. S. Farley, B. L. Gallagher, C. T. Foxon, M. Sawicki, T. Dietl, M. B. Nardelli, and J. Bernholc, Phys. Rev. Lett. **92**, 037201 (2004).

[22] M. B. Stone, K. C. Ku, S. J. Potashnik, B. L. Sheu, N. Samarth, and P. Schiffer, Appl. Phys. Lett. **83**, 4568 (2003).

[23] D. Chiba, K. Takamura, F. Matsukura, and H. Ohno, Appl. Phys. Lett. **82**, 3020 (2003).

[24] M. Adell, L. Ilver, J. Kanski, V. Stanciu, P. Svedlindh, J. Sadowski, J. Z. Domagala, F. Terki, C. Hernandez, and S. Charar, Appl. Phys. Lett. **86**, 112501 (2005).

[25] K. Takamura, F. Matsukura, D. Chiba, and H. Ohno, Appl. Phys. Lett. **81**, 2590 (2002).

[26] K. Y. Wang, M. Sawicki, K. W. Edmonds, R. P. Campion, S. Maat, C. T. Foxon, B. L. Gallagher, and T. Dietl, Phys. Rev. Lett. **95**, 217204 (2005).

[27] T. Jungwirth, K. Y. Wang, J. Mašek, K. W. Edmonds, J. König, J. Sinova, M. Polini, N. A. Goncharuk, A. H. MacDonald, M. Sawicki, A. W. Rushforth, R. P. Campion, L. X. Zhao, C. T. Foxon, and B. L. Gallagher, Phys. Rev. B **72**, 165204 (2005).

[28] K. Olejník, M. H. S. Owen, V. Novák, J. Mašek, A. C. Irvine, J. Wunderlich, and T. Jungwirth, Phys. Rev. B **78**, 054403 (2008).

[29] O. Proselkov, D. Sztenkiel, W. Stefanowicz, M. Aleszkiewicz, J. Sadowski, T. Dietl, and M. Sawicki, Appl. Phys. Lett. **100**, 262405 (2012).

[30] L. G. Parratt, Phys. Rev. **95**, 359 (1954).

[31] P. F. Fewster, *X-Ray Scattering from Semiconductors* (Imperial College Press, London, 2003), p. 82, DOI: 10.1142/9781860944581_0002.

[32] P. F. Fewster, Rep. Prog. Phys. **59**, 1339 (1996).

[33] R. C. Myers, B. L. Sheu, A. W. Jackson, A. C. Gossard, P. Schiffer, N. Samarth, and D. D. Awschalom, Phys. Rev. B **74**, 155203 (2006).

[34] U. Welp, V. K. Vlasko-Vlasov, A. Menzel, H. D. You, X. Liu, J. K. Furdyna, and T. Wojtowicz, Appl. Phys. Lett. **85**, 260 (2004).

[35] T. Uemura, M. Harada, T. Akiho, K. Matsuda, and M. Yamamoto, Appl. Phys. Lett. **98**, 102503 (2011).